Strong-contrast expansions and approximations for the effective conductivity of isotropic multiphase composites

D. C. Pham and S. Torquato[a)]
Department of Chemistry and Princeton Materials Institute, Princeton University, Princeton, New Jersey 08544

(Received 27 May 2003; accepted 27 August 2003)

We extend the previous approach of one of the authors on exact strong-contrast expansions for the effective conductivity σ_e of d-dimensional two-phase composites to case of macroscopically isotropic composites consisting of N phases. The series consists of a principal reference part and a fluctuation part (a perturbation about a homogeneous reference or comparison material), which contains multipoint correlation functions that characterize the microstructure of the composite. The fluctuation term may be estimated exactly or approximately in particular cases. We show that appropriate choices of the reference phase conductivity, such that the fluctuation term vanishes, results in simple expressions for σ_e that coincide with the well-known effective-medium and Maxwell approximations for two-phase composites. We propose a simple three-point approximation for the fluctuation part, which agrees well with a number of analytical and numerical results, even when the contrast between the phases is infinite near percolation thresholds. Analytical expressions for the relevant three-point microstructural parameters for certain mixed coated and multicoated spheres assemblages (extensions of the Hashin–Shtrikman coated-spheres assemblage) are given. It is shown that the effective conductivity of the multicoated spheres model can be determined exactly.
 [DOI: 10.1063/1.1619573]

I. INTRODUCTION

The prediction of the effective properties of composite materials has a rich history[1–3] and is still an active area of research. In general, the effective properties of a composite depend on an infinite set of correlation functions that statistically characterize the medium.[4] In the case of the effective conductivity σ_e of composite materials, our concern in the present work, a number of different approximation schemes have been devised.[1,5–7] Upper and lower bounds on the effective conductivity have been derived using variational principles.[8–13] For those composites in which the variations in the phase conductivities are small, formal solutions to the boundary-value problem have been developed in the form of weak contrast perturbation series.[14,10] Due to the nature of the integral operator, one must contend with conditionally convergent integrals, which can be made convergent using an *ad hoc* normalization procedure.[15] Alternatively, Brown[16] constructed a strong-contrast expansion of the effective conductivity of three-dimensional two-phase isotropic media in powers of rational functions of the phase conductivities.

The strong-contrast expansion approach has been further developed for the effective conductivity of d-dimensional macroscopically anisotropic composites consisting of two isotropic phases by introducing an integral equation for the cavity intensity field.[4,17,18] The expansions are not formal but rather the nth-order tensor coefficients are given explicitly in terms of integrals over products of certain tensor fields and a determinant involving n-point statistical correlation functions that render the integrals absolutely convergent in the infinite-volume limit. Thus, no renormalization analysis is required because the procedure used to solve the integral equation systematically leads to absolutely convergent integrals. Another useful feature of the expansions is that they can provide accurate estimates for all volume fractions when truncated at finite order, even when the phase conductivities differ significantly.

In this paper, we extend the strong-contrast expansion approach of Torquato[4] to the case of macroscopically isotropic composites consisting of N isotropic phases. The series expansions, which perturb about a homogeneous reference material, involve a principal reference term and a fluctuation term that perturbs about the reference medium. Based on a specified level of correlation information about the microstructure of the composite, we devise accurate approximations for the effective conductivity by choosing an appropriate equation for the conductivity of the reference (comparison) material, a free parameter in the theory. The approximation is tested against available benchmark analytical and numerical results for various models of dispersions. We find that the approximation generally provides very good agreement with these benchmark results.

In Sec. II, we derive strong-contrast expansion for the effective conductivity of macroscopically isotropic multicomponent composites. Approximation schemes based on the expansion are constructed in Sec. III, including a three-point approximation, i.e., one that contains microstructural parameters that depends on three-point corelation functions. Section IV investigates the restrictions upon the three-point parameters. Section V collects well-known three-point bounds for comparison with our three-point approximation.

a)Author to whom correspondence should be addressed; electronic mail: torquato@princeton.edu

Our three-point approximation is applied to a number of coated spheres and dispersion models and is compared with simulation results and bounds in Sec. VI.

II. STRONG-CONTRAST EXPANSIONS

We derive strong-contrast expansions of the scalar effective conductivity of a macroscopically isotropic multiphase composite. The derivation is a direct and straightforward extension of the one given by Torquato[4] for a macroscopically anisotropic two-phase composite. The reader is referred to this reference for greater details of the derivation.

Consider a large macroscopically isotropic composite specimen in arbitrary space dimension d comprised of N isotropic phases having conductivities σ_α and volume fractions $\phi_\alpha\,(\alpha=1,...,N)$. The microstructure is perfectly general but possesses a characteristic microscopic length scale that is much smaller than that of the specimen. Thus, the specimen is virtually statistically homogeneous. Ultimately, we shall take the infinite-volume limit and hence consider statistically homogeneous media. The local scalar conductivity at position $\mathbf{x}$ is expressible as

$$\sigma(\mathbf{x})=\sum_{\alpha=1}^{N}\sigma_\alpha\mathcal{I}^{(\alpha)}(\mathbf{x}), \tag{1}$$

where

$$\mathcal{I}^{(\alpha)}(\mathbf{x})=\begin{cases}1, & \mathbf{x}\ \text{in phase}\ \alpha,\\ 0, & \text{otherwise}\end{cases} \tag{2}$$

is the indicator function for phase $\alpha\,(\alpha=1,...,N)$. For statistically homogeneous media, the ensemble average of the indicator function is equal to the phase volume fraction ϕ_α, i.e.,

$$\langle\mathcal{I}^{(\alpha)}(\mathbf{x})\rangle=\phi_\alpha, \tag{3}$$

where angular brackets denote an ensemble average. The local conductivity $\sigma(\mathbf{x})$ is the coefficient of proportionality in the linear constitutive relation

$$\mathbf{J}(\mathbf{x})=\sigma(\mathbf{x})\mathbf{E}(\mathbf{x}), \tag{4}$$

where $\mathbf{J}(\mathbf{x})$ denotes the local electric (thermal) current or flux at position $\mathbf{x}$, and $\mathbf{E}(\mathbf{x})$ denotes the local field intensity. Under steady-state conditions with no source terms, conservation of energy requires that $\mathbf{J}(\mathbf{x})$ be solenoidal

$$\nabla\cdot\mathbf{J}(\mathbf{x})=0, \tag{5}$$

while the intensity field $\mathbf{E}(\mathbf{x})$ is taken to be irrotational

$$\nabla\times\mathbf{E}(\mathbf{x})=0, \tag{6}$$

which implies the existence of a potential field $T(\mathbf{x})$, i.e.,

$$\mathbf{E}(\mathbf{x})=-\nabla T(\mathbf{x}). \tag{7}$$

Thus $\mathbf{E}(\mathbf{x})$ and $T(\mathbf{x})$ represent the electric field (negative of temperature gradient) and electric potential (temperature) in the electrical (thermal) problem, respectively.

Now, following Torquato,[4] let us embed this d-dimensional composite specimen in an infinite reference phase having conductivity σ_0, which is subjected to an applied electric field $\mathbf{E}_0(\mathbf{x})$ at infinity. Introducing the polarization field defined by

$$\mathbf{P}(\mathbf{x})=[\sigma(\mathbf{x})-\sigma_0]\mathbf{E}(\mathbf{x}) \tag{8}$$

enables us to reexpress the flux $\mathbf{J}$, defined by Ohm's law (4), as follows:

$$\mathbf{J}(\mathbf{x})=\sigma_0\mathbf{E}(\mathbf{x})+\mathbf{P}(\mathbf{x}). \tag{9}$$

The vector $\mathbf{P}(\mathbf{x})$ is the induced flux polarization field relative to the reference medium.

Using the infinite-space Green's function of the Laplace equation for the reference medium corresponding to the problem, Eqs. (4)–(7), we find that the electric field satisfies the integral relation[4]

$$\mathbf{E}(\mathbf{x})=\mathbf{E}_0(\mathbf{x})+\int d\mathbf{x}'\,\mathbf{G}^{(0)}(\mathbf{r})\cdot\mathbf{P}(\mathbf{x}'), \tag{10}$$

where

$$\mathbf{G}^{(0)}(\mathbf{r})=-\mathbf{D}^{(0)}\delta(\mathbf{r})+\mathbf{H}^{(0)}(\mathbf{r}), \tag{11}$$

$$\mathbf{D}^{(0)}=\frac{1}{d\sigma_0}\mathbf{I},\quad \mathbf{H}^{(0)}(\mathbf{r})=\frac{1}{\Omega\sigma_0}\frac{d\mathbf{nn}-\mathbf{I}}{r^d}, \tag{12}$$

$\mathbf{r}=\mathbf{x}-\mathbf{x}'$, $\mathbf{n}=\mathbf{r}/|\mathbf{r}|$, $\delta(\mathbf{r})$ is the delta Dirac function, $\mathbf{I}$ is the second order identity tensor, $\Omega(d)$ is the total solid angle contained in a d-dimensional sphere given by

$$\Omega(d)=\frac{2\pi^{d/2}}{\Gamma(d/2)}, \tag{13}$$

and $\Gamma(x)$ is the gamma function. In particular, $\Omega(2)=2\pi$, $\Omega(3)=4\pi$. In relation (11), the constant second order tensor $\mathbf{D}^{(0)}$ arises because of the exclusion of the spherical cavity, and it is understood that integrals involving the second order tensor $\mathbf{H}^{(0)}$ are to be carried out by excluding at $\mathbf{x}'=\mathbf{x}$ an infinitesimal sphere in the limit that the sphere radius shrinks to zero. Moreover, the integral of $\mathbf{H}^{(0)}(\mathbf{r})$ over the surface of a sphere of radius $R>0$ is identically zero, i.e.,

$$\int_{r=R}\mathbf{H}^{(0)}(\mathbf{r})\,d\Omega=0. \tag{14}$$

Substitution of Eq. (11) into expression (10) yields an integral equation for the cavity intensity field $\mathbf{F}(\mathbf{x})$

$$\mathbf{F}(\mathbf{x})=\mathbf{E}_0(\mathbf{x})+\int_\epsilon d\mathbf{x}'\,\mathbf{H}^{(0)}(\mathbf{x}-\mathbf{x}')\cdot\mathbf{P}(\mathbf{x}'), \tag{15}$$

where we define

$$\int_\epsilon d\mathbf{x}'\,f(\mathbf{x},\mathbf{x}')=\lim_{\epsilon\to0}\int_{|\mathbf{x}-\mathbf{x}'|>\epsilon}d\mathbf{x}'\,f(\mathbf{x},\mathbf{x}'). \tag{16}$$

The cavity intensity field $\mathbf{F}(\mathbf{x})$ is related to $\mathbf{E}(\mathbf{x})$ through the expression

$$\mathbf{F}(\mathbf{x})=\{\mathbf{I}+\mathbf{D}^{(0)}[\sigma(\mathbf{x})-\sigma_0]\}\cdot\mathbf{E}(\mathbf{x}). \tag{17}$$

Combination of the expressions (8) and (17) gives a relation between the polarization and cavity intensity fields

$$\mathbf{P}(\mathbf{x})=L(\mathbf{x})\mathbf{F}(\mathbf{x}), \tag{18}$$

where

$$L(\mathbf{x})=\sigma_0 d\,\frac{\sigma(\mathbf{x})-\sigma_0}{\sigma(\mathbf{x})+(d-1)\sigma_0}=\sigma_0\, d\sum_{\alpha=1}^{N} b_{\alpha 0}\mathcal{I}^{(\alpha)}(\mathbf{x}),$$
$$b_{\alpha 0}=\frac{\sigma_\alpha-\sigma_0}{\sigma_\alpha+(d-1)\sigma_0}, \tag{19}$$

and we have used Eqs. (1) and (2).

The effective conductivity σ_e for the macroscopically isotropic composite can be defined through an expression relating the average polarization to the average Lorentz field, i.e.,

$$\langle \mathbf{P}(\mathbf{x})\rangle=\mathbf{L}_e\cdot\langle \mathbf{F}(\mathbf{x})\rangle, \tag{20}$$

where

$$\mathbf{L}_e=L_e\mathbf{I},\quad L_e=\sigma_0 d\,\frac{\sigma_e-\sigma_0}{\sigma_e+(d-1)\sigma_0}. \tag{21}$$

The constitutive relation (20) is localized, i.e., it is independent of the shape of the composite specimen in the infinite-volume limit. This relation is completely equivalent to the averaged Ohm's law that defines the effective conductivity

$$\langle \mathbf{J}(\mathbf{x})\rangle=\sigma_e\langle \mathbf{E}(\mathbf{x})\rangle. \tag{22}$$

We want to obtain an expression for the effective conductivity σ_e from relation (22) using the solution of the integral Eq. (15), which is recast as

$$\mathbf{F}(1)=\mathbf{E}_0(1)+\int_\epsilon d2\,\mathbf{H}^{(0)}(1,2)\cdot\mathbf{P}(2), \tag{23}$$

where we have adopted the shorthand notation of representing $\mathbf{x}$ and $\mathbf{x}'$ by 1 and 2, respectively. In schematic operator form, this integral equation can be tersely rewritten as

$$\mathbf{F}=\mathbf{E}_0+\mathbf{H}^{(0)}\mathbf{P}. \tag{24}$$

Multiplying this relation by the scalar $L(\mathbf{x})$ defined by Eq. (19), yields

$$\mathbf{P}=L\mathbf{E}_0+L\mathbf{H}^{(0)}\mathbf{P}. \tag{25}$$

A solution for the polarization $\mathbf{P}$ in term of the applied field $\mathbf{E}_0$ can be obtained by successive substitutions using Eq. (25), with the result

$$\mathbf{P}=L\mathbf{E}_0+L\mathbf{H}^{(0)}L\mathbf{E}_0+L\mathbf{H}^{(0)}L\mathbf{H}^{(0)}L\mathbf{E}_0+\ldots=\mathbf{S}\mathbf{E}_0, \tag{26}$$

where the second-order tensor operator $\mathbf{S}$ is given by

$$\mathbf{S}=L(\mathbf{I}-L\mathbf{H}^{(0)})^{-1}. \tag{27}$$

Ensemble averaging Eq. (26) gives

$$\langle \mathbf{P}\rangle=\langle \mathbf{S}\rangle\mathbf{E}_0. \tag{28}$$

The operator $\langle\mathbf{S}\rangle$ involves products of the tensor $\mathbf{H}^{(0)}$, which decays to zero like r^{-d} for large r, and hence $\langle\mathbf{S}\rangle$ at best involves conditionally convergent integrals. In other words, $\langle\mathbf{S}\rangle$ is dependent upon the shape of the composite specimen. In order to obtain a local (shape-independent) relation between average polarization $\langle\mathbf{P}\rangle$ and average Lorentz field $\langle\mathbf{F}\rangle$ as prescribed by Eq. (22), we must eliminate the applied field $\mathbf{E}_0$ in favor of the appropriate average field. Inverting Eq. (28) yields $\mathbf{E}_0=\langle\mathbf{S}\rangle^{-1}\langle\mathbf{P}\rangle$. Averaging Eq. (24) and eliminating the applied field $\mathbf{E}_0$ yields

$$\langle \mathbf{F}\rangle=\mathbf{Q}\langle\mathbf{P}\rangle, \tag{29}$$

where

$$\mathbf{Q}=\langle\mathbf{S}\rangle^{-1}+\mathbf{H}^{(0)}. \tag{30}$$

Comparing expressions (20) and (29) yields the desired result for the effective tensor $\mathbf{L}_e$:

$$\mathbf{L}_e^{-1}=\mathbf{Q}=\mathbf{H}^{(0)}+\langle\mathbf{S}\rangle^{-1}=\mathbf{H}^{(0)}+\langle L(\mathbf{I}-L\mathbf{H}^{(0)})^{-1}\rangle^{-1}. \tag{31}$$

The first few terms of the expansion Eq. (31) are explicitly given by

$$\mathbf{L}_e^{-1}(1)=\int d2\,\mathbf{Q}(1,2)=\frac{\mathbf{I}(1)}{\langle L(1)\rangle}-\int d2\left(\frac{\langle L(1)L(2)\rangle-\langle L(1)\rangle\langle L(2)\rangle}{\langle L(1)\rangle\langle L(2)\rangle}\right)\mathbf{H}^{(0)}(1,2)$$
$$-\int\int d2\,d3\left(\frac{\langle L(1)L(2)L(3)\rangle}{\langle L(1)\rangle\langle L(2)\rangle}-\frac{\langle L(1)L(2)\rangle\langle L(2)L(3)\rangle}{\langle L(1)\rangle\langle L(2)\rangle\langle L(3)\rangle}\right)\mathbf{H}^{(0)}(1,2)\cdot\mathbf{H}^{(0)}(2,3)-\ldots \tag{32}$$

The general term contains the n-point correlation functions $\langle L(1)\ldots L(n)\rangle$. The explicit expression for any term in the series can be given as in Ref. 4.

Let us introduce the property-independent dipole tensor

$$\mathbf{t}(\mathbf{r})=\sigma_0\mathbf{H}^{(0)}(\mathbf{r})=\frac{d\mathbf{n}\mathbf{n}-\mathbf{I}}{\Omega r^d}. \tag{33}$$

Substituting Eqs. (19) and (33) into Eq. (32) and taking into account that $\mathbf{t}$ is traceless, we take the trace of both sides of Eq. (32). We then multiply them with $\sigma_0(\Sigma_\alpha\phi_\alpha b_{\alpha 0})^2$ to obtain the relation for our macroscopically isotropic media

$$\frac{\sigma_e+(d-1)\sigma_0}{\sigma_e-\sigma_0}\left(\sum_\alpha \phi_\alpha b_{\alpha 0}\right)^2-\sum_\alpha \phi_\alpha b_{\alpha 0}$$
$$=\mathcal{A}(\sigma_0,\sigma_1,\ldots,\sigma_N,\text{microstructure}). \tag{34}$$

Here $\mathcal{A}(\sigma_0,\sigma_1,\ldots,\sigma_N,\text{microstructure})$ is a scalar quantity that depends on the reference conductivity σ_0, phase conductivities $\sigma_1,\ldots,\sigma_N$, and the microstructure via n-point correlation functions. The left side of Eq. (34) is referred to as the principal reference term of the strong-contrast expansion, while the right side, given by $\mathcal{A}$ is the fluctuation term relative to the reference medium of conductivity σ_0. Through the lowest three-point term in the series, $\mathcal{A}$ is explicitly given by

$$\mathcal{A}(\sigma_0,\sigma_1,\ldots,\sigma_N,\text{microstructure}) = -d\Bigg[\sum_{\alpha,\beta,\gamma} b_{\alpha 0}b_{\beta 0}b_{\gamma 0}\int\int d2\,d3\langle \mathcal{I}^{(\alpha)}(1)t_{ij}(1,2)\mathcal{I}^{(\beta)}(2)t_{ij}(2,3)\mathcal{I}^{(\gamma)}(3)\rangle - \sum_{\alpha,\beta,\gamma,\delta}\frac{b_{\alpha 0}b_{\beta 0}b_{\gamma 0}b_{\delta 0}}{\Sigma_\kappa \phi_\kappa b_{\kappa 0}}\int\int d2\,d3\langle \mathcal{I}^{(\alpha)}(1)t_{ij}(1,2)\mathcal{I}^{(\beta)}(2)\rangle\langle \mathcal{I}^{(\gamma)}(2)t_{ij}(2,3)\mathcal{I}^{(\delta)}(3)\rangle\Bigg] - \ldots . \tag{35}$$

Here conventional summation on repeating Latin indices (from 1 to d) is assumed, and the Greek indices under the sum run from 1 to N.

III. APPROXIMATION SCHEMES

A. Connections to previous estimates

The effective medium approximation (EMA) σ_{EMA} (also known as the self-consistent scheme)[5,7] is the solution of the equation

$$\sum_{\alpha=1}^{N}\phi_\alpha\frac{\sigma_\alpha-\sigma_{\text{EMA}}}{\sigma_\alpha+(d-1)\sigma_{\text{EMA}}}=0. \tag{36}$$

Equivalently, we can rewrite this via the property function P_σ

$$\sigma_e=\sigma_{\text{EMA}}=P_\sigma((d-1)\sigma_{\text{EMA}}), \tag{37}$$

where

$$P_\sigma(\sigma_*)=\left[\sum_{\alpha=1}^{N}\frac{\phi_\alpha}{\sigma_\alpha+\sigma_*}\right]^{-1}-\sigma_*. \tag{38}$$

This approximation is exact for a certain hierarchical composite consisting of spherical grains.[19] As $\sigma_0\to\sigma_{\text{EMA}}$ (while $\sigma_e=\sigma_{\text{EMA}}$), the left-hand side of Eq. (34) approaches 0, and hence for the EMA microstructure we have

$$\mathcal{A}(\sigma_e,\sigma_1,\ldots,\sigma_N,\text{EMA microstructure})=0. \tag{39}$$

For two-phase microstructures that are optimal when the volume fraction is specified, such as the Hashin–Shtrikman coated-spheres assemblage,[8] we have

$$\sigma_e=P_\sigma[(d-1)\sigma_M], \tag{40}$$

where σ_M is the property of the connected matrix phase in the optimal geometry. Thus Eq. (34) also yields

$$\mathcal{A}(\sigma_M,\sigma_1,\sigma_2,\text{optimal two-phase microstructure})=0. \tag{41}$$

Formula (40) is sometimes called the Maxwell approximation (MA) (also known as the Maxwell–Garnett or Clausius–Mossotti approximation).

B. Multipoint approximations

The fluctuation term $\mathcal{A}$ depends on the microstructure of the composite and generally can only be evaluated by some numerical scheme. Torquato[17] used the strong-contrast expansion to develop a three-point approximation (henceforth referred to as TPA1) for the effective conductivity of two-phase composites that can be regarded to perturb about the Hashin–Shtrikman structures[4]

$$\frac{\sigma_e}{\sigma_1}=\frac{1+(d-1)\phi_2 b_{21}-(d-1)\phi_1\zeta_2 b_{21}^2}{1-\phi_2 b_{21}-(d-1)\phi_1\zeta_2 b_{21}^2}\quad\text{(TPA1)}, \tag{42}$$

where ζ_α is a three-point microstructural parameter defined by Eqs. (48) and (49). Here the reference phase is taken to be phase 1.

We will now derive a different three-point approximation for multiphase composites based on the results Eqs. (36)–(41). Let us assume that we have an explicit approximation $\mathcal{A}_{\text{approx}}$ for the fluctuation term $\mathcal{A}$ for a specific composite. Guided by the discussion of Sec. III A, our strategy is to choose σ_0 to be the solution of the equation $\mathcal{A}_{\text{approx}}=0$, and from Eq. (34) deduce the respective approximation $\sigma_e=P_\sigma[(d-1)\sigma_0]$. Let us assume that $\mathcal{A}_{\text{approx}}=\mathcal{A}_n$, where $\mathcal{A}_n$ is the series $\mathcal{A}$ truncated after the n-point correlation term. From Eq. (34), we deduce the respective n-point approximation for the effective conductivity

$$\sigma_e=P_\sigma((d-1)\sigma_0),\quad \mathcal{A}_n(\sigma_0)=0. \tag{43}$$

Clearly, at $n\to\infty$, we should get the exact value of the effective conductivity for an arbitrary microstructure. For any microstructure, we expect that σ_0 should lie within the interval $[\sigma_{\min},\sigma_{\max}]$ for σ_e in order to satisfy the Hashin–Shtrikman bounds,[8] which can be expressed as

$$P_\sigma((d-1)\sigma_{\max})\geqslant\sigma_e\geqslant P_\sigma((d-1)\sigma_{\min}), \tag{44}$$

where

$$\sigma_{\max}=\max\{\sigma_1,\ldots,\sigma_N\},\quad \sigma_{\min}=\min\{\sigma_1,\ldots,\sigma_N\}. \tag{45}$$

For example, let us take $\mathcal{A}_{\text{approx}}=\mathcal{A}_3$. Since three-point microstructural information is now available for a variety of different microstructures, we are especially interested in the three-point approximation (TPA2):

$$\sigma_e=P_\sigma((d-1)\sigma_0)\quad\text{(TPA2)}, \tag{46}$$

where σ_0 is the solution of equation

$$\mathcal{A}_3(\sigma_0)=0. \tag{47}$$

We call this TPA2 to distinguish it from TPA1 given by Eq. (42). Both three-point approximations are exact through third order in the difference in the phase conductivities.

In the special two-phase case, three-point correlation function information arises via the microstructural parameters $\zeta_\alpha(\alpha=1,2)$,[4,20,21] which for $d=2$

$$\zeta_\alpha=\frac{4}{\pi\phi_1\phi_2}\int_0^\infty\frac{dr}{r}\int_0^\infty\frac{ds}{s}\int_0^\pi d\theta\cos(2\theta)\left[S_3^{(\alpha)}(r,s,t)-\frac{S_2^{(\alpha)}(r)S_2^{(\alpha)}(s)}{S_1^{(\alpha)}}\right], \tag{48}$$

and for $d=3$

$$\zeta_\alpha=\frac{9}{2\phi_1\phi_2}\int_0^\infty\frac{dr}{r}\int_0^\infty\frac{ds}{s}\int_{-1}^1 d(\cos\theta)\times P_2(\cos\theta)\left[S_3^{(\alpha)}(r,s,t)-\frac{S_2^{(\alpha)}(r)S_2^{(\alpha)}(s)}{S_1^{(\alpha)}}\right], \tag{49}$$

where P_2 is the Legendre polynomial of order 2 and θ is the angle opposite the side of the triangle of length t, and

$$S_n^{(\alpha)}(\mathbf{x}_1,\cdots,\mathbf{x}_n)=\langle\mathcal{I}^{(\alpha)}(\mathbf{x}_1)\cdots\mathcal{I}^{(\alpha)}(\mathbf{x}_n)\rangle. \tag{50}$$

It is also known[4,20,21] that $\zeta_1\geqslant 0$, $\zeta_2\geqslant 0$, and $\zeta_1+\zeta_2=1$. Through the microstructural parameters ζ_1 and ζ_2, relation (47) can be given simply as

$$\zeta_1\frac{\sigma_1-\sigma_0}{\sigma_1+(d-1)\sigma_0}+\zeta_2\frac{\sigma_2-\sigma_0}{\sigma_2+(d-1)\sigma_0}=0. \tag{51}$$

We can further simplify Eq. (47) for $N\geqslant 2$. According to the ergodic hypothesis, we could substitute the ensemble averages in Eq. (35) by volume averages over the volume of the macroscopic sample V, which we can take for convenience to be spherical. Thus, for a statistically homogeneous and isotropic medium of spherical volume V, we have

$$\int\langle\mathcal{I}^{(\alpha)}(\mathbf{x})t_{ij}(\mathbf{x},\mathbf{y})\mathcal{I}^{(\beta)}(\mathbf{y})\rangle d\mathbf{y}=\int_V\int_V\mathcal{I}^{(\alpha)}(\mathbf{x})t_{ij}(\mathbf{x},\mathbf{y})\mathcal{I}^{(\beta)}(\mathbf{y})d\mathbf{x}\,d\mathbf{y}=0. \tag{52}$$

Then Eq. (47) can be written as

$$\sum_{\alpha,\beta,\gamma}b_{\alpha0}b_{\beta0}b_{\gamma0}A_\beta^{\alpha\gamma}=0, \tag{53}$$

where

$$A_\beta^{\alpha\gamma}=\int_V\int_V\int_V d1\,d2\,d3\mathcal{I}^{(\alpha)}(1)t_{ij}(1,2)\mathcal{I}^{(\beta)}(2)\times t_{ij}(2,3)\mathcal{I}^{(\gamma)}(3). \tag{54}$$

Note the symmetry of $A_\beta^{\alpha\gamma}$ in the indices α and γ, but not in β. The sum on the left side of Eq. (53) is of quadratic form in the variables $b_{\alpha0}$, $b_{\gamma0}$ $(\alpha,\gamma=1,...,N)$, the sign of which depends on those of $b_{\beta0}$ $(\beta=1,...,N)$. Hence, at $\sigma_0=\sigma_{\min}$, the sum is positive, while at $\sigma_0=\sigma_{\max}$, it is negative, with the solution σ_0 of Eq. (53) lying between these extreme values. Consequently, the TPA2 from Eqs. (46) and (53) should always fall inside the Hashin–Shtrikman bounds Eq. (44). For $N=2$, the microstructural parameters ζ_α is related to $A_\alpha^{\alpha\alpha}$ via

$$A_\alpha^{\alpha\alpha}=\frac{d-1}{d}\phi_1\phi_2\zeta_\alpha,\quad \alpha=1,2. \tag{55}$$

C. Alternative approaches

We note that $\mathbf{L}_e$ of Eq. (31) can also be expanded as

$$(\mathbf{L}_e^{-1}-\mathbf{H}^{(0)})^{-1}=\langle\mathbf{S}\rangle=\langle L(\mathbf{I}-L\mathbf{H}^{(0)})^{-1}\rangle=\langle L\rangle\mathbf{I}+\sum_{n=1}^\infty\langle L(L\mathbf{H}^{(0)})^n\rangle, \tag{56}$$

where we have used an obvious short-hand notation in the second line of Eq. (56). If we take σ_0 such that the last sum in Eq. (56) vanishes, then we deduce

$$(\mathbf{L}_e^{-1}-\mathbf{H}^{(0)})^{-1}=\langle L\rangle\mathbf{I}\rightarrow\mathbf{L}_e^{-1}=\mathbf{H}^{(0)}+\langle L\rangle^{-1}\mathbf{I}. \tag{57}$$

In the same manner as that of the previous section, we obtain the expression

$$\sigma_e=P_\sigma((d-1)\sigma_0), \tag{58}$$

where σ_0 is the solution of the equation

$$\hat{\mathcal{A}}(\sigma_0,\sigma_1,\ldots,\sigma_N,\text{microstructure})=0, \tag{59}$$

$$\hat{\mathcal{A}}=\sum_{n=2}^\infty d^n\sum_{\alpha_1,\ldots,\alpha_n}b_{\alpha_1 0}b_{\alpha_2 0}\ldots b_{\alpha_n 0}\int\cdots\int d2\ldots dn\times\langle\mathcal{I}^{(\alpha_1)}(1)t_{ij}(1,2)\mathcal{I}^{(\alpha_2)}(2)\ldots t_{li}(n-1,n)\mathcal{I}^{(\alpha_n)}(n)\rangle. \tag{60}$$

At the three-point approximation level, Eqs. (58)–(60) leads to the same result Eqs. (46) and (53) of the previous subsection.

Moreover we see that Eq. (31) can also be given as

$$\mathbf{L}_e(\mathbf{I}-\mathbf{L}_e\mathbf{H}^{(0)})^{-1}=\langle L(\mathbf{I}-L\mathbf{H}^{(0)})^{-1}\rangle, \tag{61}$$

which can be expanded as

$$\mathbf{L}_e\left[\mathbf{I}+\sum_{k=1}^\infty\langle(L_e\mathbf{H}^{(0)})^k\rangle\right]=\langle L\rangle\mathbf{I}+\sum_{k=1}^\infty\langle L(L\mathbf{H}^{(0)})^k\rangle. \tag{62}$$

Taking nth approximation of Eq. (62) gives

$$\mathbf{L}_e\left[\mathbf{I}+\sum_{k=1}^{n-1}\langle(L_e\mathbf{H}^{(0)})^k\rangle\right]=\langle L\rangle\mathbf{I}+\sum_{k=1}^{n-1}\langle L(L\mathbf{H}^{(0)})^k\rangle. \tag{63}$$

If we take σ_0 as to make the last sum of the right-hand of Eq. (63) vanish [c.f. Eqs. (59) and (60)], then at the three-point approximation, Eq. (63) leads to the same result Eqs. (46) and (53).

IV. THREE-POINT MICROSTRUCTURAL PARAMETERS

As in the two-phase case, there exist some relations between the microstructural parameters $A_\beta^{\alpha\gamma}$. From Eq. (54), we see that they are symmetric in the indices α and γ. Consider a spherical representative element V of the composite with phase α occupying regions V_α $(\alpha=1,...,N)$. For simplicity and without loss of generality we take the volume of V to be unity, and hence the volume of V_α is equal to the volume fraction ϕ_α. Let us introduce the harmonic potentials

$$\varphi(\mathbf{x})=\int_V G(\mathbf{x}-\mathbf{y})d\mathbf{y},\quad \boldsymbol{\nabla}^2\varphi(\mathbf{x})=1,\quad \mathbf{x}\in V; \tag{64}$$

$$\varphi^{\alpha}(\mathbf{x})=\int_{\phi\alpha} G(\mathbf{x}-\mathbf{y})d\mathbf{y}, \quad \nabla^2\varphi^{\alpha}(\mathbf{x})=\delta_{\alpha\beta}, \quad \mathbf{x}\in\phi_{\beta}; \tag{65}$$

where $G(r)$ $(r=|\mathbf{x}-\mathbf{y}|)$ is the respective Green function

$$G(r)=\begin{cases} -\dfrac{1}{2\pi}\ln\left(\dfrac{1}{r}\right), & d=2 \\ -\dfrac{1}{(d-2)\Omega}\dfrac{1}{r^{d-2}}, & d\geqslant 3 \end{cases}, \quad \nabla^2 G=\delta(r). \tag{66}$$

We have

$$G_{,ij}=\frac{\delta_{ij}}{d}\,\delta(\mathbf{x}-\mathbf{y})-t_{ij}, \qquad t_{ij}=\frac{dn_in_j-\delta_{ij}}{\Omega r^d}, \quad n_i=\frac{x_i-y_i}{r}, \tag{67}$$

where the Latin indices after a comma designate differentiation with respective to position. If we denote

$$\varphi^{\alpha}_{ij}(\mathbf{x})=\varphi^{\alpha}_{,ij}-\frac{1}{d}\,\delta_{ij}\delta_{\alpha\beta}, \quad \mathbf{x}\in\phi_{\beta}, \tag{68}$$

then we have

$$A^{\alpha\gamma}_{\beta}=\int_{V_{\beta}}\varphi^{\alpha}_{ij}\varphi^{\gamma}_{ij}d\mathbf{x}=\int_V\int_V\int_V d\mathbf{x}\,d\mathbf{y}\,d\mathbf{z}\mathcal{I}^{(\alpha)}(\mathbf{x}) \times t_{ij}(\mathbf{x},\mathbf{y})\mathcal{I}^{(\beta)}(\mathbf{y})t_{ij}(\mathbf{y},\mathbf{z})\mathcal{I}^{(\gamma)}(\mathbf{z}). \tag{69}$$

Note that

$$\varphi_{,ij}=\frac{\delta_{ij}}{d}=\sum_{\alpha=1}^{N}\varphi^{\alpha}_{,ij}, \tag{70}$$

and hence we find that

$$\int_{V_{\gamma}}\varphi_{,ij}\varphi^{\beta}_{,ij}d\mathbf{x}=\int_{V_{\gamma}}\frac{1}{d}\,\varphi^{\beta}_{,ii}d\mathbf{x}=\frac{\delta_{\beta\gamma}}{d}\,\phi_{\gamma}, \tag{71}$$

and

$$\begin{aligned}\int_{V_{\gamma}}\varphi_{,ij}\varphi^{\beta}_{,ij}d\mathbf{x}&=\sum_{\alpha=1}^{N}\int_{V_{\gamma}}\varphi^{\alpha}_{,ij}\varphi^{\beta}_{,ij}d\mathbf{x}\\&=\sum_{\alpha=1}^{N}\int_{V_{\gamma}}\left[\varphi^{\alpha}_{ij}\varphi^{\beta}_{ij}+\frac{1}{d}\,\delta_{\alpha\gamma}\delta_{\beta\gamma}\right]d\mathbf{x}\\&=\sum_{\alpha=1}^{N}A^{\alpha\beta}_{\gamma}+\frac{\delta_{\beta\gamma}}{d}\,\phi_{\gamma}.\end{aligned} \tag{72}$$

Comparing Eqs. (71) and (72), we obtain relations between the microstructural parameters

$$\sum_{\alpha=1}^{N}A^{\alpha\beta}_{\gamma}=0, \quad \forall\beta,\gamma=1,...,N. \tag{73}$$

In the two-component case Eq. (73) yields

$$A^{11}_1=A^{22}_1=-A^{12}_1, \quad A^{11}_2=A^{22}_2=-A^{12}_2. \tag{74}$$

Keeping in mind Eq. (55) and $\zeta_1+\zeta_2=1$, we have

$$A^{11}_1+A^{22}_2=\frac{d-1}{d}\,\phi_1\phi_2. \tag{75}$$

Generally, a N-phase material with microstructural parameters $A^{\alpha\gamma}_{\beta}(\alpha,\gamma,\beta=1,...,N)$ can also be considered to be a two-phase material occupying regions $V_{\mathrm{I}}=\cup_{\alpha\in\Gamma_{\mathrm{I}}}V_{\alpha}$, $V_{\mathrm{II}}=\cup_{\alpha\in\Gamma_{\mathrm{II}}}V_{\alpha}$ with respective microstructural parameters $\overline{A}^{\alpha\gamma}_{\beta}(\alpha,\gamma,\beta=\mathrm{I,II})$. Here $\Gamma_{\mathrm{I}}=\{\alpha_1,...,\alpha_k\}$, $\Gamma_{\mathrm{II}}=\{\alpha_{k+1},...,\alpha_N\}$, and $\{\alpha_1,...,\alpha_k,\alpha_{k+1},...,\alpha_N\}$ is any permutation of $\{1,...,N\}$, and k is any number between 1 and $N-1$. By combining the relations Eqs. (65), (68), (69), and (75), one can verify that

$$\begin{aligned}&\frac{d-1}{d}\left(\sum_{\alpha\in\Gamma_{\mathrm{I}}}\phi_{\alpha}\right)\left(\sum_{\alpha\in\Gamma_{\mathrm{II}}}\phi_{\alpha}\right)\\&=\frac{d-1}{d}\,\overline{\phi}_{\mathrm{I}}\overline{\phi}_{\mathrm{II}}=\overline{A}^{\mathrm{I}}_{\mathrm{I}}{}^{\mathrm{I}}+\overline{A}^{\mathrm{II}}_{\mathrm{II}}{}^{\mathrm{II}}\\&=\sum_{\beta,\gamma,\alpha\in\Gamma_{\mathrm{I}}}A^{\alpha\gamma}_{\beta}+\sum_{\beta,\gamma,\alpha\in\Gamma_{\mathrm{II}}}A^{\alpha\gamma}_{\beta},\end{aligned} \tag{76}$$

where $\overline{\phi}_{\mathrm{I}}$ and $\overline{\phi}_{\mathrm{II}}$ are the volume fractions of regions I and II, respectively.

V. THREE-POINT BOUNDS

Here we summarize previous three-point bounds that we will subsequently apply. The d-dimensional three-point Beran bounds[14] for two-phase composites derived by Torquato[4] are given by

$$\sigma^{(3U)}\geqslant\sigma_e\geqslant\sigma^{(3L)}, \tag{77}$$

where

$$\sigma^{(3U)}=\sigma_1\phi_1+\sigma_2\phi_2-\frac{\phi_1\phi_2(\sigma_1-\sigma_2)^2}{\sigma_1\phi_2+\sigma_2\phi_1+(d-1)(\sigma_1\zeta_1+\sigma_2\zeta_2)}, \tag{78}$$

$$\sigma^{(3L)}=\sigma_1\phi_1+\sigma_2\phi_2-\frac{\phi_1\phi_2(\sigma_1-\sigma_2)^2}{\sigma_1\phi_2+\sigma_2\phi_1+(d-1)(\zeta_1/\sigma_1+\zeta_2/\sigma_2)^{-1}}. \tag{79}$$

Milton[22] obtained a sharper lower bound for the case $d=3$ and $\sigma_2\geqslant\sigma_1$

$$\sigma^{(3L)}/\sigma_1=\frac{1+(1+2\phi_2)b_{21}-2(\phi_1\zeta_2-\phi_2)b^2_{21}}{1+\phi_1 b_{21}-(2\phi_1\zeta_2+\phi_2)b^2_{21}}, \qquad b_{21}=\frac{\sigma_2-\sigma_1}{\sigma_2+2\sigma_1}. \tag{80}$$

For three-dimensional N-phase composites, Phan-Thien and Milton[10] derive the following bounds:

$$\sigma^{(3U)}\geqslant\sigma_e\geqslant\sigma^{(3L)}, \tag{81}$$

where

$$\sigma^{(3U)}=\langle\sigma\rangle-\delta\sigma\cdot\mathbf{\Gamma}\cdot(\mathbf{\Gamma}+\delta\sigma\cdot\mathbf{A}/\langle\sigma\rangle)^{-1}\cdot\mathbf{\Gamma}\cdot\delta\sigma/3\langle\sigma\rangle, \tag{82}$$

$$1/\sigma^{(3L)}=\langle\sigma^{-1}\rangle-2\,\delta\sigma^{-1}\cdot\mathbf{\Gamma}\cdot(\mathbf{\Gamma}+\delta\sigma^{-1}\cdot(\mathbf{\Delta}+\mathbf{A})/2\langle\sigma^{-1}\rangle)^{-1}\cdot\mathbf{\Gamma}\cdot\delta\sigma^{-1}/3\langle\sigma^{-1}\rangle, \tag{83}$$

with $(N-1)$-rank vectors and matrices

$$\delta\sigma=\{\sigma_\alpha-\sigma_N\}_{\alpha=1}^{N-1},\quad \delta\sigma^{-1}=\{\sigma_\alpha^{-1}-\sigma_N^{-1}\}_{\alpha=1}^{N-1},$$

$$\mathbf{\Gamma}=\{\Gamma_{\alpha\beta}\}_{\alpha,\beta=1}^{N-1},\quad \mathbf{A}=\{A_{\alpha\beta\gamma}\}_{\alpha,\beta,\gamma=1}^{N-1}, \tag{84}$$

$$\mathbf{\Delta}=\{\Delta_{\alpha\beta\gamma}\}_{\alpha,\beta,\gamma=1}^{N-1},\quad \Gamma_{\alpha\beta}=\begin{cases}\phi_\alpha(1-\phi_\alpha), & \alpha=\beta\\ -\phi_\alpha\phi_\beta, & \alpha\neq\beta;\end{cases} \tag{85}$$

$$\Delta_{\alpha\beta\gamma}=\begin{cases}(1-2\phi_\beta)\Gamma_{\beta\gamma}, & \alpha=\beta\\ -\phi_\alpha\Gamma_{\beta\gamma}-\phi_\beta\Gamma_{\alpha\gamma}, & \alpha\neq\beta.\end{cases}$$

Here $\langle f(\sigma)\rangle$ for any function f of σ is given by

$$\langle f(\sigma)\rangle=\sum_{\alpha=1}^{N}\phi_\alpha f(\sigma_\alpha). \tag{86}$$

The PhanThien–Milton microstructural parameters $A_{\alpha\beta\gamma}$ can be related to our $A_\alpha^{\beta\gamma}$ via the expression

$$\begin{aligned}A_{\alpha\beta\gamma}&=\frac{1}{16\pi^2}\int\int\frac{d\mathbf{r}\,d\mathbf{s}}{rs}\left(\frac{\partial^2}{\partial\mathbf{r}\partial\mathbf{s}}\right)^2\langle\Omega'_\alpha(\mathbf{0})\Omega'_{\boldsymbol{\beta}}(\mathbf{r})\Omega'_\gamma(\mathbf{s})\rangle\\&=\int_V\int_V\int_V d\mathbf{x}\,d\mathbf{y}\,d\mathbf{z}(\mathcal{I}^{(\beta)}(\mathbf{x})-\phi_\beta)G_{,ij}(\mathbf{x},\mathbf{y})(\mathcal{I}^{(\alpha)}(\mathbf{y})-\phi_\alpha)G_{,ij}(\mathbf{y},\mathbf{z})(\mathcal{I}^{(\gamma)}(\mathbf{z})-\phi_\gamma)\\&=A_\alpha^{\beta\gamma}-\phi_\alpha\sum_{\delta=1}^{N}A_\delta^{\beta\gamma}+\frac{1}{3}(\phi_\alpha\delta_{\alpha\beta}\delta_{\alpha\gamma}-\phi_\alpha\phi_\beta\delta_{\beta\gamma}-\phi_\beta\phi_\gamma\delta_{\alpha\gamma}-\phi_\alpha\phi_\gamma\delta_{\beta\alpha}+2\phi_\alpha\phi_\beta\phi_\gamma).\end{aligned} \tag{87}$$

Three-point bounds for d-dimensional N-phase composites derived by Pham[13,23] are given by

$$P_\sigma((d-1)\sigma_0^{(3U)})\geqslant\sigma_e\geqslant P_\sigma((d-1)\sigma_0^{(3L)}), \tag{88}$$

where $\sigma_0^{(3U)}$ and $\sigma_0^{(3L)}$ are the solutions of the equations

$$\begin{aligned}&Q_\sigma^{(3U)}((d-1)\sigma_0^{(3U)})=0,\\&Q_\sigma^{(3L)}((d-1)\sigma_0^{(3L)})=0,\end{aligned} \tag{89}$$

$$Q_\sigma^{(3U)}((d-1)\sigma_0)=\sum_{\alpha,\beta,\gamma}(\sigma_\alpha-\sigma_0)A_\alpha^{\beta\gamma}X_\beta X_\gamma, \tag{90}$$

$$Q_\sigma^{(3L)}((d-1)\sigma_0)=\sum_{\alpha,\beta,\gamma}(\sigma_\alpha^{-1}-\sigma_0^{-1})A_\alpha^{\beta\gamma}X_\beta X_\gamma, \tag{91}$$

$$X_\beta=\langle[\sigma+(d-1)\sigma_0]^{-1}\rangle-[\sigma_\beta+(d-1)\sigma_0]^{-1}. \tag{92}$$

In the two-phase case, relations (89) are solved explicitly as

$$\sigma_0^{(3U)}=\frac{\sigma_1A_1^{11}+\sigma_2A_2^{22}}{A_1^{11}+A_2^{22}}=\zeta_1\sigma_1+\zeta_2\sigma_2, \tag{93}$$

$$\sigma_0^{(3L)}=\frac{A_1^{11}+A_2^{22}}{A_1^{11}/\sigma_1+A_2^{22}/\sigma_2}=(\zeta_1/\sigma_1+\zeta_2/\sigma_2)^{-1}. \tag{94}$$

If we imagine a fictitious composite with ζ_1 and ζ_2 being the volume fractions of the phases, then $\sigma_0^{(3U)}$ and $\sigma_0^{(3L)}$ in Eqs. (93) and (94) are, respectively, the ''arithmetic'' and ''harmonic'' averages. Moreover, the solution σ_0 of Eq. (51) is the ''effective medium approximation'' value, hence $\sigma_0^{(3U)}\geqslant\sigma_0\geqslant\sigma_0^{(3L)}$, and consequently the three-point approximation $P_\sigma(\sigma_0)$ from Eqs. (46) and (51) should fall inside the three-point bounds Eqs. (88), (93), and (94) for our real composite. In the two-phase case, the bounds Eqs. (88), (93), and (94) as well as the bounds Eqs. (81)–(83) coincide with the bounds Eqs. (77)–(79).

The bounds Eqs. (81)–(83), and (88) and (89) have been compared in Ref. 24 for the class of N-phase ($N\geqslant3$) quasi-symmetric (symmetric cell) materials using a symbolic algebra program and numerical simulation. It appears that the bounds yield the same results for N-phase spherical cell materials. For N-phase platelet cell materials, the bounds Eqs. (81)–(83) appear tighter. However, the bounds Eqs. (88) and (89) are simpler in functional form as well as computational aspects. In the case of N-phase spherical cell composites, Eq. (89) are also solved explicitly and yield $\sigma_0^{(3U)}=\langle\sigma\rangle$, $\sigma_0^{(3L)}=\langle\sigma^{-1}\rangle^{-1}$. Unsuccessful attempts have been made to transform Eqs. (81)–(83), which involve multiplications and inversions of $(N-1)$-rank matrices and vectors, into some simple form similar to that of Eqs. (88) and (89).

VI. APPLICATIONS OF THE THREE-POINT APPROXIMATION

In this section, we apply our three-point approximation (TPA2) to certain multicoated spheres assemblages and dispersions of identical spheres. In each of these instances, the relevant three-point microstructural parameters are known.

A. Analytical two-phase models

There are only very few nontrivial models, in which the three-point microstructural parameters $A_\alpha^{\beta\gamma}$ have been deter-

mined analytically. Here we discuss three such instances. For the two-phase EMA microstructure,[19,22] we have

$$\zeta_1=\phi_1, \quad \zeta_2=\phi_2. \tag{95}$$

With Eq. (95), we see that relation (51) for σ_0 has the identical form as Eq. (36) for σ_{EMA} in the two-phase case. Hence our TPA2 Eqs. (46) and (51) coincides with the exact value Eq. (37) for two-phase EMA microstructure, i.e.,

$$\sigma_{\mathrm{TPA}}=P_\sigma((d-1)\sigma_0)=\sigma_{\mathrm{EMA}}=P_\sigma((d-1)\sigma_{\mathrm{EMA}}). \tag{96}$$

Thus, in the two-phase case, our TPA2 Eqs. (46) and (51) may be interpreted as a three-point generalization of EMA, while the classical EMA expression Eq. (37) is the corresponding two-point version.

Next, consider the Hashin–Shtrikman two-phase coated spheres model, which consists of composite spheres that are composed of a spherical core, of conductivity σ_2, and radius a, surrounded by a concentric shell of conductivity σ_1 and outer radius b. The ratio $(a/b)^3$ is fixed and equal to the inclusion volume fraction ϕ_2. The composite spheres fill all space, implying that there is a distribution in their sizes ranging to the infinitely small [see Fig. 1(a)]. For this coated spheres model, $A_\alpha^{\beta\gamma}$ have been determined explicitly,[25] which for general d-dimensional composites can be given as

$$\begin{aligned} &A_1^{11}=A_1^{22}=-A_1^{12}=\frac{d-1}{d}\phi_1\phi_2, \\ &A_2^{11}=A_2^{22}=-A_2^{12}=0. \end{aligned} \tag{97}$$

Hence, from Eq. (55) one finds

$$\zeta_1=1, \quad \zeta_2=0. \tag{98}$$

Consequently, from Eqs. (93) and (94), one obtains $\sigma_0^{(3U)}=\sigma_0^{(3L)}=\sigma_1$, and the bounds Eq. (88) coincide to yield the exact effective conductivity

$$\sigma_e=P_\sigma((d-1)\sigma_1). \tag{99}$$

This relation coincides with the Maxwell approximation and Hashin–Shtrikman upper bound (when $\sigma_2<\sigma_1$) or lower bound (when $\sigma_2>\sigma_1$). The result Eq. (99) was also obtained by direct solution of the respective conductivity problem,[8] which in turn leads to Eq. (98). Relation (99) is also realizable by certain laminates[4] and thus are also optimal. With Eq. (98), the solution of Eq. (51) should be $\sigma_0=\sigma_1$, and from Eq. (46) we get the same formula Eq. (99). Thus, for two-phase coated spheres (as well as other optimal models), our three-point approximation also coincides with the exact result.

A generalization of the Hashin–Shtrikman coated-spheres model is the mixed-coated-spheres model.[26] This microstructure consists of a mixture of the two types of coated spheres corresponding to the Hasin–Shtrikman upper and lower bounds at a fixed volume fraction. Thus, an additional parameter is the proportion of coated spheres in which phase α is the included phase and phase $\beta(\neq\alpha)$ is the matrix, which we denotes by $\phi_{\alpha\beta}$. Clearly, $\phi_{12}+\phi_{21}=\phi_1+\phi_2=1$. For this geometry [Fig. 1(b)], the microstructural parameters have been determined analytically.[26] The d-dimensional generalizations are given by

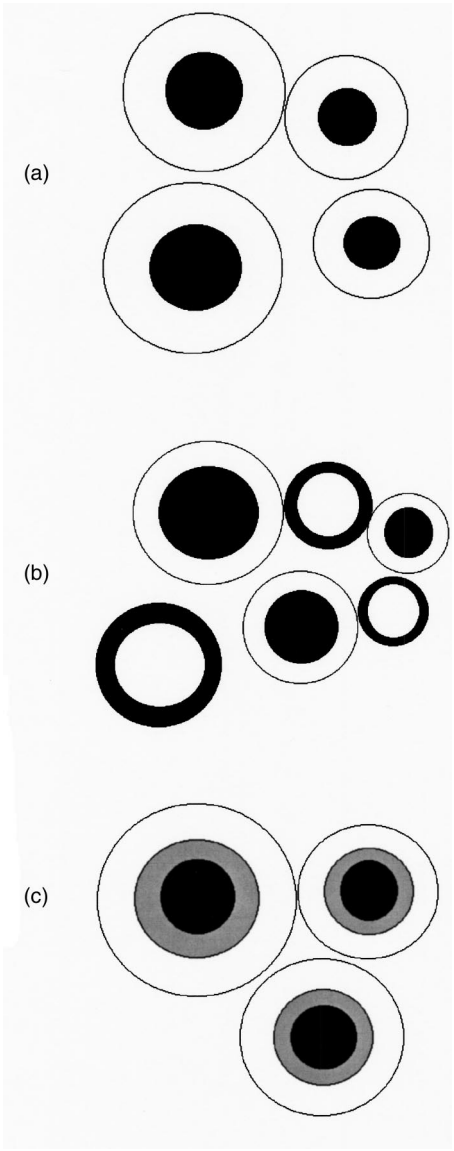

FIG. 1. Schematic illustrations of three different coated-spheres models: (a) Hashin–Shtrikman two-phase coated-spheres assemblage; (b) two-phase mixed-coated-spheres assemblage; and (c) multiphase doubly coated spheres assemblage.

$$\begin{aligned} &A_1^{11}=A_1^{22}=-A_1^{12}=\frac{d-1}{d}\phi_1\phi_2\phi_{21}, \\ &A_2^{11}=A_2^{22}=-A_2^{12}=\frac{d-1}{d}\phi_1\phi_2\phi_{12}, \end{aligned} \tag{100}$$

and from Eq. (55)

$$\zeta_1=\phi_{21}, \quad \zeta_2=\phi_{12}. \tag{101}$$

As an example, consider the case $\sigma_2/\sigma_1=20$. The Hashin–Shtrikman (HS) bounds Eq. (44), three-point (TP) bounds Eqs. (78) and (80), and the three-point approximation (TPA2) Eqs. (46) and (51) are compared in the plane σ_e/σ_1 versus ϕ_2 [see Fig. 2(a)]. In Fig. 2(b), the three-point approximation is plotted versus ϕ_{21} in the range $0\leqslant\phi_{21}\leqslant1$, the extreme cases corresponding to the Hashin–Shtrikman's upper and lower bounds, respectively.

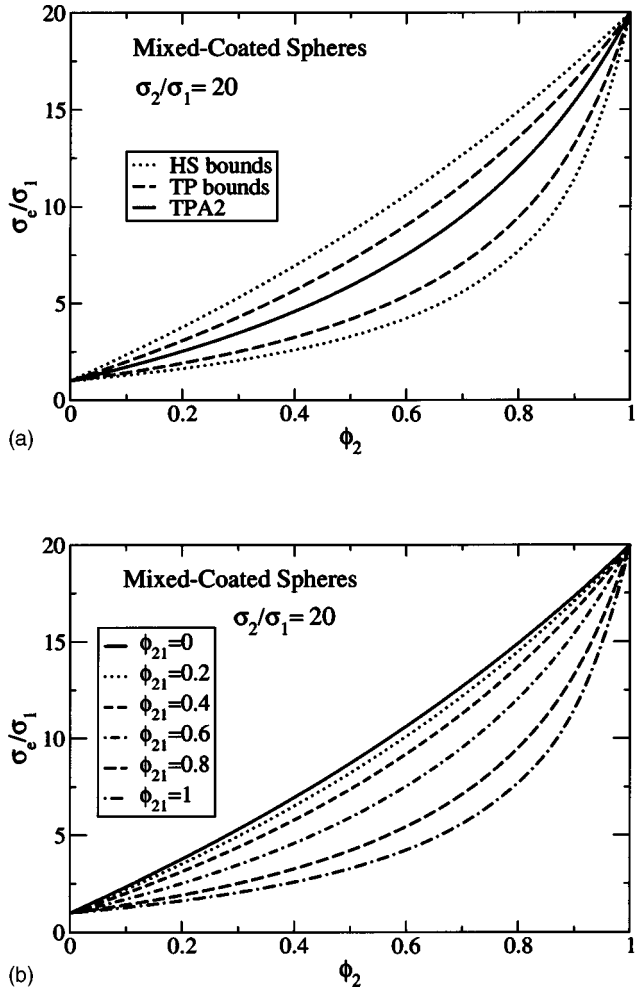

FIG. 2. (a) Comparison of the three-point approximation (TPA2) (solid curve) for a two-phase mixed-coated-spheres model for $\sigma_2/\sigma_1=20$, $\phi_{21}=0.6$ to the HS bounds (dotted curves) and the TP bounds (dashed curves). (b) The TPA2 for the mixed-coated-spheres model for a range of ϕ_{21} with $\sigma_2/\sigma_1=20$.

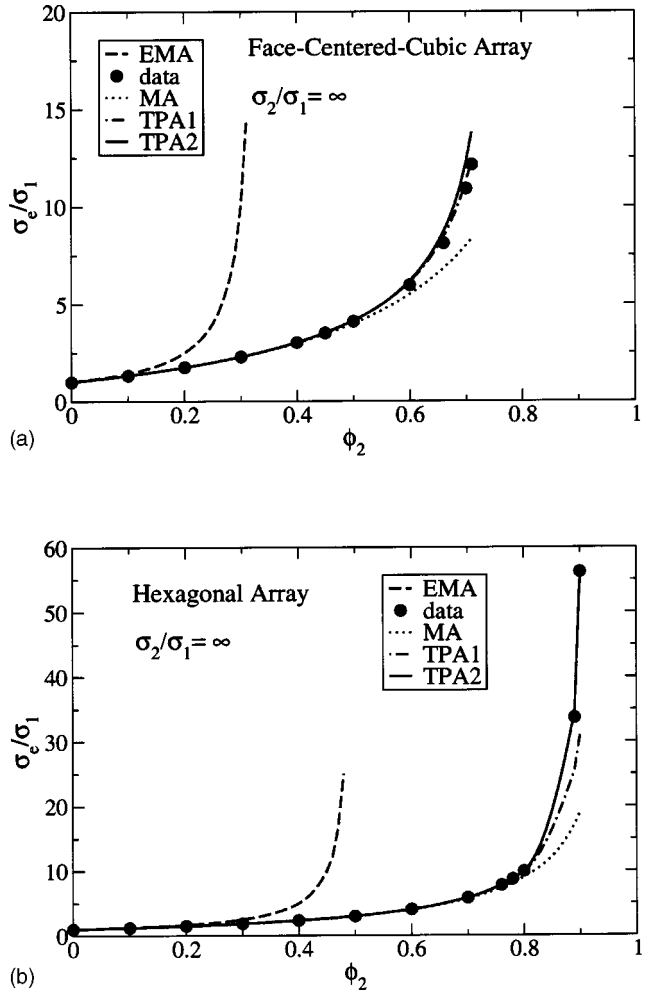

FIG. 3. Comparison of simulation data (Refs. 32 and 33) for the effective conductivity of equisized ordered superconducting particles to relations (37), (40), (42), and (46) for the EMA, MA, TPA1, and TPA2, respectively: (a) face-centered-cubic spheres (Ref. 32) and (b) hexagonal array of aligned circular cylinders (see Ref. 33).

B. Periodic and random dispersions of spheres

Here we apply our approximation to various periodic and random dispersions of spheres. The three-point microstructural parameters ζ_α for these models are available in the literature.[4,27–37] We consider the infinite-phase contrast cases: superconducting inclusions in a normal conductor ($\sigma_2/\sigma_1=\infty$) and perfectly insulating inclusions in a normal conductor ($\sigma_2/\sigma_1=0$). These are the most stringent test of our approximation. Relation (51) in these instances yields

$$\sigma_0=\begin{cases}\sigma_1/(1-d\zeta_2) & \text{if } \zeta_2\leqslant\dfrac{1}{d}\\ \infty \quad \text{if } \zeta_2\geqslant\dfrac{1}{d}\end{cases},$$

$$(\sigma_2/\sigma_1=\infty), \tag{102}$$

$$\sigma_0=\begin{cases}\left(1-\dfrac{d}{d-1}\zeta_2\right)\sigma_1 & \text{if } \zeta_2\leqslant\dfrac{d-1}{d}\\ 0 \quad \text{if } \zeta_2\geqslant\dfrac{d-1}{d}\end{cases},$$

$$(\sigma_2/\sigma_1=0). \tag{103}$$

Interestingly, our approximation predicts a nontrivial microstructure-dependent percolation threshold. For the superconducting and perfectly insulating cases, it predicts a percolation threshold at $\zeta_{2c}=1/d$ and $\zeta_{2c}=(d-1)/d$, respectively. The corresponding threshold in terms of volume fraction ϕ_{2c} is easily found from the function $\zeta_2(\phi_2)$ tabulated in the aforementioned literature. One cannot expect a three-point approximation to yield accurate estimates of the percolation threshold, which requires higher-order microstructural (clustering) information. It is interesting to note, however, that for some two-dimensional (rather than three-dimensional cases), Eqs. (102) and (103) yield reasonable estimates of ϕ_{2c}. For example, for a two-dimensional square array, Eq. (102) predicts $\phi_{2c}\approx 0.775$, which is to be compared to the exact result $\phi_{2c}=\pi/4\approx 0.785$.

The predictions of our TPA2 for the effective conductivity are compared to simulation data for certain periodic dispersions[32,33] [see Figs. 3(a) and 3(b)] and random dispersions[34–37] [see Figs. 4(a), 4(b), and 5] over large ranges of volume fractions ϕ_2. We include in the figures relations (37), (40), and (42) for the EMA, MA, and TPA1, respectively. We see that both the TPA1 and TPA2 are rela-

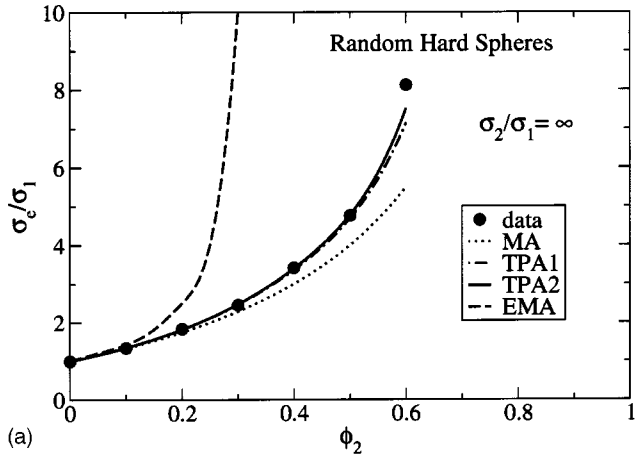

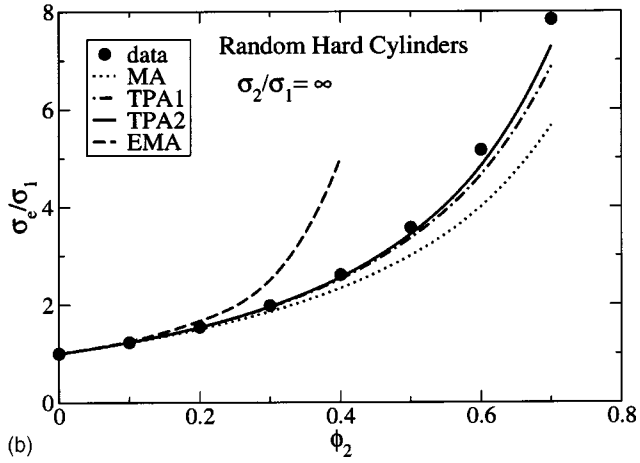

FIG. 4. Comparison of simulation data (see Refs. 34–36) for the effective conductivity of equisized random superconducting particles to relations (37), (40), (42), and (46) for the EMA, MA, TPA1, and TPA2, respectively: (a) random dispersions of hard spheres (see Ref. 35), and (b) random dispersions of hard circular cylinders (see Refs. 34 and 36).

tively good predictors of σ_e up to high volume fractions ϕ_2 of the included phase close to the percolation threshold, where higher-order information is clearly required to be more accurate. For superconducting cases in three dimensions, the TPA1 is slightly more accurate than the TPA2 for the ordered array but the reverse is true for the disordered array. For superconducting cases in two dimensions, the TPA1 and TPA2 are comparable, except at high volume fractions where the TPA2 is more accurate. In the case of perfectly insulating overlapping spheres, the TPA1 and TPA2 are again comparable, but the TPA2 is superior at high sphere volume fractions. The TPA2 is most accurate for simple periodic systems, followed by random dispersions of hard cylinders and spheres, and least accurate for overlapping cylinders and spheres.

C. Multicoated spheres

Another generalization of the Hashin–Shtrikman two-phase coated-spheres assemblage is the *N*-phase multicoated spheres model.[26] Here spheres of phase 1 are coated with spherical shells of phase 2, which in turn are coated with spherical shells of phase 3,... [see Fig. 1(c)]. The relative

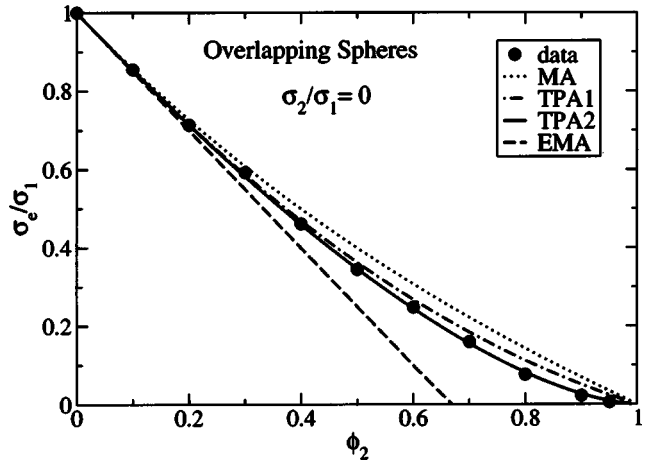

FIG. 5. Comparison of simulation data (see Ref. 37) for the effective conductivity of equisized random dispersions of overlapping insulating spheres to relations (37), (40), (42), and (46) for the EMA, MA, TPA1, and TPA2, respectively.

volume proportions and coating orders of the phases in all *N*-compound spheres are the same. The microstructural parameters of this *N*-phase model have also been determined exactly,[26] which in *d*-dimensional space can be expressed as $(\alpha,\beta,\gamma=1,...,N)$

$$
\begin{aligned}
&A_\alpha^{\beta\gamma}=\frac{d-1}{d}\,\phi_\alpha\phi_\beta\phi_\gamma\Bigg(\sum_{\delta<\alpha}\phi_\delta\cdot\sum_{\kappa\leqslant\alpha}\phi_\kappa\Bigg)^{-1},\\
&\beta,\gamma<\alpha;\\
&A_\alpha^{\alpha\beta}=-\frac{d-1}{d}\,\phi_\alpha\phi_\beta\Bigg(\sum_{\delta\leqslant\alpha}\phi_\delta\Bigg)^{-1},\quad \beta<\alpha;\\
&A_\alpha^{\alpha\alpha}=\frac{d-1}{d}\,\phi_\alpha\sum_{\delta<\alpha}\phi_\delta\cdot\Bigg(\sum_{\kappa\leqslant\alpha}\phi_\kappa\Bigg)^{-1},\quad \alpha\geqslant 2;\\
&A_\alpha^{\beta\gamma}=0\quad \text{if } \beta>\alpha \text{ or } \gamma>\alpha \text{ or } \alpha=\beta=\gamma=1.
\end{aligned}
\tag{104}
$$

For example, for the three-phase doubly-coated spheres in three dimensions, Eq. (104) becomes

$$
\begin{aligned}
&A_1^{11}=A_1^{2\alpha}=A_1^{3\alpha}=A_2^{3\alpha}=0,\quad \alpha=1,2,3\\
&A_2^{22}=A_2^{11}=-A_2^{12}=\tfrac{2}{3}\phi_1\phi_2(\phi_1+\phi_2)^{-1},\\
&A_3^{33}=\tfrac{2}{3}\phi_3(\phi_1+\phi_2),\quad A_3^{13}=-\tfrac{2}{3}\phi_1\phi_3,\\
&A_3^{23}=-\tfrac{2}{3}\phi_2\phi_3,\quad A_3^{12}=\tfrac{2}{3}\phi_1\phi_2\phi_3(\phi_1+\phi_2)^{-1},\\
&A_3^{11}=\tfrac{2}{3}\phi_1^2\phi_3(\phi_1+\phi_2)^{-1},\quad A_3^{22}=\tfrac{2}{3}\phi_2^2\phi_3(\phi_1+\phi_2)^{-1},
\end{aligned}
\tag{105}
$$

while Eq. (87) yields

$$
\begin{aligned}
&A_{111}=\tfrac{1}{3}(\phi_1-3\phi_1^2+2\phi_1^3)-\phi_1(A_2^{11}+A_3^{11}),\\
&A_{222}=\tfrac{1}{3}(\phi_2-3\phi_2^2+2\phi_2^3)+A_2^{22}-\phi_2(A_2^{22}+A_3^{22}),\\
&A_{112}=\tfrac{1}{3}(2\phi_1^2\phi_2-\phi_1\phi_2)-\phi_1(A_2^{12}+A_3^{12}),\\
&A_{211}=\tfrac{1}{3}(2\phi_1^2\phi_2-\phi_1\phi_2)+A_2^{11}-\phi_2(A_2^{11}+A_3^{11}),\\
&A_{212}=\tfrac{1}{3}(2\phi_2^2\phi_1-\phi_1\phi_2)+A_2^{12}-\phi_2(A_2^{12}+A_3^{12}),\\
&A_{122}=\tfrac{1}{3}(2\phi_2^2\phi_1-\phi_1\phi_2)-\phi_1(A_2^{22}+A_3^{22}).
\end{aligned}
\tag{106}
$$

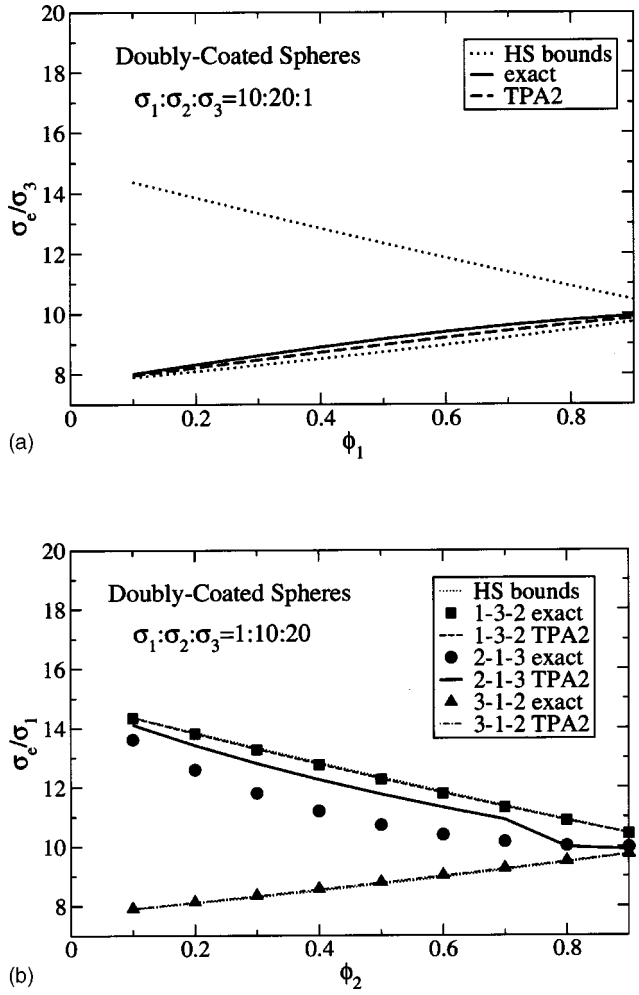

FIG. 6. Comparison of exact effective conductivity values to the HS bounds Eq. (44) and the TPA2 Eq. (46) for a three-phase doubly coated spheres model: (a) $\sigma_1=10\sigma_3$, $\sigma_2=20\sigma_3$, $\phi_1=0.1\rightarrow 0.9$, $\phi_2=\frac{4}{5}(1-\phi_1)$, $\phi_3=\frac{1}{5}(1-\phi_1)$, conventional coating order 1-2-3 (phase 1 in phase 2 in phase 3) and (b) $\sigma_2=10\sigma_1$, $\sigma_3=20\sigma_1$, $\phi_2=0.1\rightarrow 0.9$, $\phi_1=\frac{1}{5}(1-\phi_2)$, $\phi_3=\frac{4}{5}(1-\phi_2)$, for coating orders: 1-3-2 (phase 1 embedded in phase 3, and then in phase 2), 2-1-3, and 3-1-2.

For numerical illustrations, we take $\sigma_1=10\sigma_3$, $\sigma_2=20\sigma_3$, $\phi_1=0.1\rightarrow 0.9$, $\phi_2=\frac{4}{5}(1-\phi_1)$, $\phi_3=\frac{1}{5}(1-\phi_1)$, conventional coating order 1-2-3 (phase 1, then phase 2, then phase 3). The HS bounds Eq. (44), TP bounds Eqs. (81)–(83), and TPA2 Eqs. (46) and (53) are plotted in Fig. 6(a). It is interesting to find that the TP bounds Eqs. (81)–(83) with relations (105) and (106) concide to yield the exact effective conductivity of the doubly coated spheres model.

In Table I, we take $\sigma_2=10\sigma_1$, $\sigma_3=20\sigma_1$ ($\sigma_1<\sigma_2<\sigma_3$), $\phi_2=0.1\rightarrow 0.9$, $\phi_1=\frac{1}{5}(1-\phi_2)$, $\phi_3=\frac{4}{5}(1-\phi_2)$, and collect the exact effective conductivity values of the doubly coated spheres model at different coating orders: 1-3-2, 1-2-3, 2-1-3, 2-3-1, 3-2-1, and 3-1-2. The HS upper (HSU) and lower HS (HSL) bounds are also given for comparison. Some of these results are plotted in Fig. 6(b) together with the respective TPA2 results (46) and (53). It is interesting to observe that the model with highest conductivity is 1-3-2 (but not 1-2-3), and the model with lowest conductivity is 3-1-2 (not 3-2-1), in which the matrix phases are not the ones with extremal conductivities. Note also that most of the exact and approximation values are close to the Hashin–Shtrikman upper or lower bounds, except those for the model 2-1-3, which falls between the bounds.

The fact that TP bounds Eqs. (81)–(83) with relations (105) and (106) yield exact effective conductivities for doubly coated spheres that do not coincide with the TPA2 value indicates that our TPA2 Eqs. (46) and (53) is not as accurate for general *N*-phase composites as for two-phase ones. The TPA2 does not always yield the best possible approximation and it may even violate certain three-point bounds using the same available geometric information (although it always falls within the two-point Hashin–Shtrikman bounds as confirmed). Therefore, in the general *N*-phase case, this approximation should be used in conjunction with bounds. One can use computer simulation to verify that TP bounds Eqs. (81)–(83) with relations (87) and (104) converge to yield the exact effective conductivity of general *N*-phase multicoated spheres.

We can also generalize the model further: consider a random mixture of multicoated spheres of different kinds, each of which has different coating order. The only restriction is that the volume proportions of the constituent materials in all of the compound spheres are the same. For such generalized models, the three-point microstructural parameters $A_\alpha^{\beta\gamma}$ can also be determined explicitly, however the TP bounds Eqs. (81)–(83) generally should not converge, as evidenced by the two-phase mixed-coated-spheres model considered.

TABLE I. Exact effective conductivities for doubly coated spheres models at various embedding orders, and HSU and HSL bounds. Here we take $\sigma_2=10\sigma_1$, $\sigma_3=20\sigma_1$ ($\sigma_1<\sigma_2<\sigma_3$), $\phi_2=0.1\rightarrow 0.9$, $\phi_1=\frac{1}{5}(1-\phi_2)$, $\phi_3=\frac{4}{5}(1-\phi_2)$.

ϕ_2	HSU	1-3-2	1-2-3	2-1-3	2-3-1	3-2-1	3-1-2	HSL
0.1	14.377	14.348	14.248	13.616	8.014	7.988	7.919	7.895
0.2	13.853	13.804	13.673	12.601	8.318	8.266	8.136	8.092
0.3	13.339	13.277	13.146	11.809	8.614	8.538	8.356	8.296
0.4	12.835	12.765	12.649	11.197	8.897	8.802	8.580	8.510
0.5	12.340	12.270	12.174	10.735	9.163	9.053	8.807	8.732
0.6	11.855	11.789	11.715	10.399	9.404	9.288	9.038	8.963
0.7	11.378	11.322	11.270	10.170	9.615	9.504	9.273	9.205
0.8	10.911	10.869	10.837	10.034	9.789	9.697	9.511	9.458
0.9	10.451	10.428	10.414	9.981	9.920	9.864	9.754	9.723

VII. CONCLUSIONS

In this article, exact strong-contrast expansions for the effective conductivity σ_e of d-dimensional macroscopically isotropic composites consisting of N phases are presented. The series consists of a principal reference part and a fluctuation part, which contains multipoint correlation functions that characterize the microstructure of the composite. The fluctuation term may be estimated exactly or approximately in particular cases using available information about the given microstructure. We demonstrate that appropriate choices of the reference phase conductivity, such that this fluctuation term vanishes, results in simple expressions for σ_e that agree with the well-known two-phase estimates. We propose a simple three-point approximation for the fluctuation part, which agrees well with a number of analytical and numerical results, including those for the EMA and HS coated-spheres microstructures, and various periodic and random dispersions of spheres and aligned cylinders. Even when the contrast between the phases is infinite, the approximation can yield accurate predictions, sometimes up to the percolation thresholds. In cases where clustering effects are significant, higher-order percolation information may be needed for the effective conductivity to be described accurately. We have also given the analytical expressions of the three-point correlation parameters for certain mixed-coated and multicoated spheres assemblages. It is shown that the effective conductivity of the multicoated spheres model can be determined explicitly from known three-point bounds and exact values of the respective three-point parameters.

ACKNOWLEDGMENTS

The work was completed during D. C. P.'s visit to the Materials Institute, Princeton University as a Fulbright Senior Scholar. S. T. was supported by a MRSEC Grant at Princeton University, Grant No. NSF DMR-0213706 and by the Air Force Office of Scientific Research under Grant No. F49620-03-1-0406.

[1] J. C. Maxwell, *A Treatise on Electricity and Magnetism* (Clarendon, Oxford, 1892).
[2] Lord Rayleigh, Philos. Mag. **34**, 481 (1892).
[3] A. Einstein, Ann. Phys. (Leipzig) **19**, 289 (1906).
[4] S. Torquato, *Random Heterogeneous Materials* (Springer, New York, 2002).
[5] D. A. G. Bruggeman, Ann. Phys. (Leipzig) **24**, 636 (1935).
[6] R. Landauer, J. Appl. Phys. **23**, 779 (1952).
[7] R. Landauer, in *Electrical Transport and Optical Properties of Inhomogeneous Media*, edited by J. C. Garland and D. B. Tanner (AIP, New York, 1978).
[8] Z. Hashin and S. Shtrikman, J. Appl. Phys. **33**, 3125 (1962).
[9] M. J. Beran, *Statistical Continuum Theories* (Wiley, New York, 1968).
[10] N. Phan-Thien and G. W. Milton, Proc. R. Soc. London, Ser. A **380**, 333 (1982).
[11] S. Torquato, J. Chem. Phys. **84**, 6345 (1986).
[12] S. Torquato and M. D. Rintoul, Phys. Rev. Lett. **75**, 4067 (1995); **76**, 3241 (1996); R. Lipton and B. Vernescu, Proc. R. Soc. London, Ser. A **452**, 329 (1996).
[13] D. C. Pham, Arch. Ration. Mech. Anal. **127**, 191 (1994).
[14] M. J. Beran, Nuovo Cimento **38**, 771 (1965).
[15] J. J. McCoy, Q. Appl. Math. **36**, 137 (1979).
[16] W. F. Brown, J. Chem. Phys. **23**, 1514 (1955).
[17] S. Torquato, J. Appl. Phys. **58**, 3790 (1985).
[18] A. K. Sen and S. Torquato, Phys. Rev. B **39**, 4504 (1989).
[19] G. W. Milton, Commun. Math. Phys. **99**, 463 (1985).
[20] S. Torquato, Ph.D. Dissertation, State University of New York, Stony Brook, New York, 1980.
[21] G. W. Milton, Phys. Rev. Lett. **46**, 542 (1981).
[22] G. W. Milton, in *Physics and Chemistry of Porous Media*, edited by D. L. Johnson and P. N. Sen (AIP, New York, 1984).
[23] D. C. Pham, Phys. Rev. E **56**, 652 (1997).
[24] D. C. Pham and N. Phan-Thien, Z. Angew. Math **48**, 744 (1997).
[25] D. C. Pham, Mech. Mater. **27**, 249 (1998).
[26] D. C. Pham, Acta Mech. **121**, 177 (1997).
[27] R. C. McPhedran and G. W. Milton, Appl. Phys. A: Solids Surf. **26**, 207 (1981).
[28] S. Torquato, G. Stell, and J. Beasley, Int. J. Eng. Sci. **23**, 385 (1985).
[29] S. Torquato and J. D. Beasley, Int. J. Eng. Sci. **24**, 415 (1986).
[30] S. Torquato and F. Lado, Proc. R. Soc. London, Ser. A **417**, 59 (1988).
[31] C. A. Miller and S. Torquato, J. Appl. Phys. **68**, 5486 (1990).
[32] D. R. McKenzie, R. C. McPhedran, and G. H. Derrick, Proc. R. Soc. London, Ser. A **362**, 211 (1978).
[33] W. T. Perrins, D. R. McKenzie, and R. C. McPhedran, Proc. R. Soc. London, Ser. A **369**, 207 (1979).
[34] I. C. Kim and S. Torquato, J. Appl. Phys. **68**, 3892 (1990).
[35] I. C. Kim and S. Torquato, J. Appl. Phys. **69**, 2280 (1991).
[36] H. W. Cheng and L. Greengard, J. Comput. Phys. **136**, 629 (1997).
[37] I. C. Kim and S. Torquato, J. Appl. Phys. **71**, 2727 (1992).